

DMD #59410

**Hydrastine Pharmacokinetics and Metabolism after a Single Oral Dose of
Goldenseal (*Hydrastis canadensis*) to Humans.**

Prem K. Gupta, Gary Barone, Bill J. Gurley, E. Kim Fifer, and Howard P. Hendrickson

Department of Pharmaceutical Sciences, College of Pharmacy (P.K.G., B.J.G., E.K.F.,
H.P.H.), Department of Surgery, College of Medicine (G.B.) University of Arkansas for
Medical Sciences, Little Rock, AR

DMD #59410

Running title

Hydrastine ADME in Humans after a Single Dose of Goldenseal

Corresponding author

Howard P. Hendrickson, Ph.D.

Department of Pharmaceutical Sciences

College of Pharmacy

University of Arkansas for Medical Sciences #622

4301 West Markham Street

Little Rock, AR 72205

Phone: (501) 603-1547

E-mail: hendricksonhowardp@uams.edu

Document statistics

Text Pages: 18

Tables: 5

Figures: 5

References: 32

Abstract: 227

Introduction: 481

Discussion: 472

Abbreviations: CID, collision-induced-dissociation; DDA, data-dependent-acquisition;

DMD #59410

ABSTRACT:

The disposition and metabolism of hydrastine was investigated in 11 healthy subjects following oral dose of 2.7 g of Goldenseal supplement containing 78 mg hydrastine.

Serial blood samples were collected for 48 h and urine was collected for 24 h.

Hydrastine serum and urine concentrations were determined by LC-MS/MS.

Pharmacokinetic parameters for hydrastine were calculated using non-compartmental methods. Maximal serum concentration (C_{max}) was 225 ± 100 ng/ml, T_{max} was 1.5 ± 0.3 h, and AUC was 6.4 ± 4.1 ng*h/ml*kg. The elimination half-life was 4.8 ± 1.4 h.

Metabolites of hydrastine were identified in serum and urine by using liquid chromatography coupled to high-resolution mass spectrometry (LC-QToF). Hydrastine metabolites were identified by various mass spectrometric techniques such as accurate mass measurement, neutral loss scanning and product ion scanning using Q-ToF and triple quadrupole instruments. The identity of phase II metabolites was further confirmed by hydrolysis of glucuronide and sulfate conjugates using bovine β -glucuronidase and *Helix Pomatia* sulfatase/glucuronidase enzyme preparation. Hydrastine was found to undergo rapid and extensive phase I and phase II metabolism. Reduction, O-demethylation, N-demethylation, hydroxylation, aromatization, lactone hydrolysis and dehydrogenation of alcohol group formed by lactone hydrolysis to ketone group were observed during phase I biotransformation of hydrastine. Phase II metabolites were primarily glucuronide and sulfate conjugates. Hydrastine undergoes extensive biotransformation, and some metabolites may have pharmacological activity; further study is needed in this area.

DMD #59410

INTRODUCTION

Goldenseal (*Hydrastis canadensis* L.) is a popular dietary supplement in the United States touted for its antimicrobial properties and use in gastrointestinal disorders. The primary alkaloids with known biological activity are the phthalide isoquinoline alkaloid (1-*R*, 9-*S*)- β -hydrastine and the quaternary protoberberine-type alkaloid berberine (Weber et al., 2003). Goldenseal is unique from other hydrastine containing plants in that (-)- β -hydrastine is the only hydrastine isomer present, while the (+)-enantiomer is found in other hydrastine-containing plants (Blaskó et al., 1982). While a number of therapeutic activities have been attributed to berberine, the pharmacological effects of hydrastine are less studied and its safety profile is poorly understood and to frame the relevant pharmacological effects of hydrastine within the specific stereochemistry found in goldenseal.

(1*R*, 9*S*)- β -hydrastine ((-)- β -hydrastine) has been shown to have several specific biological activities including, inhibition of tyrosine hydroxylase in PC-12 cells (Yin et al., 2004), a relaxant effect on guinea pig isolated trachea, (Abdel-Haq et al., 2000) and inhibition of several cytochrome P450 (CYP) enzymes (Chatterjee and Franklin, 2003; Etheridge et al., 2007; Raner et al., 2007). Toxicological studies performed on goldenseal powder in mice and rats indicate that at commonly used doses goldenseal supplements are non-toxic, thus its constituents are likely to be safe for human use when taken at reasonable doses (Dunnick et al., 2011). Goldenseal also has the potential to produce herb-drug interactions, as it can inhibit human cytochrome P450 3A4 (CYP3A4) and CYP2D6 activity *in vivo* (Gurley et al., 2008a; Gurley et al., 2008b). It appears that both berberine and hydrastine contribute to the inhibition of human

DMD #59410

CYP3A4 and CYP2D6 (Chatterjee and Franklin, 2003; Chen et al., 2013). Chatterjee and Franklin have shown that (+) and (-) hydrastine inhibited with increasing potency CYP2D6 ($IC_{50} > 500 \mu M$), CYP2C9 ($IC_{50} 350 \mu M$), and CYP3A4 ($IC_{50} = 25 \mu M$). The potency of CYP3A4 appeared to be due primarily to hydrastine since IC_{50} for berberine was $400 \mu M$ and there was little change in the potency when the assay was conducted with goldenseal extracts containing $19 \mu M$ hydrastine. Chen and co-workers have shown that berberine inhibits chlorzoxazone and dextromethorphan metabolism implying that berberine inhibits CYP2E1 and CYP2D6, respectively (Chen et al., 2013). These investigators did not study or report results for hydrastine under similar conditions.

Despite goldenseal's widespread usage, the pharmacokinetics of hydrastine in humans has not been adequately described. While it is difficult to determine the proper dosage range for any herbal product, a recent extensive survey of the literature suggests a daily dose of Hydrastis in the range of 0.9 to 3 g per day (Blumenthal et al., 2003). In the present study, the pharmacokinetic profile and metabolism of hydrastine were studied in human subjects after administration of a single dose of 2.7 g of goldenseal supplement containing 78 mg of hydrastine. The metabolism of hydrastine in mammals has not been described in the literature, but some insight of potential metabolism can be derived from studies reported for noscapine, a phthalide tetrahydroisoquinoline alkaloid isolated from opium (Tsunoda and Yoshimura, 1979; Tsunoda and Yoshimura, 1981; Fang et al., 2012). The full scan high resolution MS (HRMS) scan at low and intermediate collision energy, data dependent acquisition with selection of ions for MS/MS scan based on neutral loss

DMD #59410

or an intensity threshold, and a scan of selected ions for obtaining structural information were used as data acquisition techniques. Metabolites were identified by extracting ion chromatograms of fragment ions characteristic of the hydrastine ion in the intermediate collision energy LC-MS runs and then looking for possible intact metabolite peaks at the same retention time. Phase II metabolites were identified by characteristic neutral loss of phase II metabolites in data-dependent-acquisition (DDA) mode.

The primary objectives of this clinical study were to determine the disposition of hydrastine following a single therapeutically relevant dose of 2.7 g of goldenseal supplement and to determine the extent of hydrastine phase I and phase II metabolism. Some conjecture of potential enzymes responsible for hydrastine is also discussed and based primarily on reported metabolism for the hydrastine analogue noscapine.

DMD #59410

MATERIALS and METHODS

Chemicals. β -hydrastine (purity 99%), noscapine (purity 97%) and formic acid (purity 98%) were purchased from Sigma-Aldrich, (St. Louis, MO). LC-MS grade methanol and acetonitrile were purchased from Fisher Scientific (Houston, TX). β -Glucuronidase Type H-1 from *Helix pomatia*, was purchased from Sigma-Aldrich (St. Louis, MO). Goldenseal supplement was purchased from Nature's Resource (Lot# 0/10184, Mission Hills, CA). This brand of Goldenseal was chosen because it was used in previous human studies conducted by our group (Gurley et al., 2007; Gurley et al., 2008b; Gupta et al., 2009) and the manufacturer (Pharmavite, LLC) claims to follow current Good Manufacturing Practices (cGMP) in the sourcing and manufacture of its products. Each goldenseal was independently determined to contain 13 mg of hydrastine. Human serum was purchased from Millipore (Bedford, MA) or Innovative Research (Novi, MI). LCMS Optima grade water was purchased from Thermo-Fisher Scientific.

Study Design. Eleven healthy adults (age 31 ± 8 years; weight 84 ± 25 kg; 11 male and 1 female) participated in a small pilot study to assess the disposition of goldenseal alkaloids. All subjects responded to questions related their medical history, were nonsmokers, ate a normal diet, were not users of botanical dietary supplements, were not taking prescription (females allowed birth control medication) or nonprescription medications. Females who were pregnant or breastfeeding were excluded from the study. Furthermore a blood sample was collected at the time of consent and data from a comprehensive metabolic panel (CMP) was used to determine the health of the potential subject prior to enrolling in the study. Subjects were asked to refrain from eating after midnight on day of the study and where provided a standardized meal 4

DMD #59410

hours after taking goldenseal. The study protocol was approved by the University of Arkansas for Medical Sciences Human Research Advisory Committee (Little Rock, AR), and all participants were provided written informed consent before commencing the study. No formal follow up with study subjects was conducted, but subjects were asked to report any abnormalities (e.g., fever, rash, difficulty breathing, or gastric distress) to the study physician or investigator.

The isoquinoline alkaloid content (hydrastine and berberine) of goldenseal was independently determined *via* the method of Abourashed and Khan by ChromaDex (Irvine, CA). (Abourashed and Khan, 2001) Six capsules (2.7 g solid dried goldenseal root powder and the daily dose recommended by the manufacturer) were administered to each subject with 8 oz. of water, while in the UAMS Clinical Research Center. This dose contained 78 mg hydrastine and 132 mg berberine. These capsules were further characterized using dissolution testing at a pH of 2.0 (0.01 M hydrochloric acid). Greater than 90% of the hydrastine was released from the capsule with the first 30 min of dissolution. A type II dissolution apparatus was used in this study that showed dissolution and solubility favorable to oral absorption. Blood samples (10 mL) were collected at pre-dose, 0.25, 0.5, 0.75, 1, 1.5, 2, 3, 4, 6, 8, 12, 24, 36, and 48 hours following goldenseal administration. Blood was allowed to clot at 4°C for at least 1 hour. Clotted blood samples were centrifuged for 10 min at 4000 rcf and the serum transferred to a clean tube for storage at -80°C. Urine was collected for 24 hours after Goldenseal administration and then stored at -80°C.

LC-MS/MS quantitation of hydrastine in serum and urine:

DMD #59410

The quantitation of hydrastine in human serum and urine was performed using a Quattro Premier triple quadrupole mass spectrometer (Waters, Milford, MA) interfaced to an Acquity UPLC system (Waters, Milford, MA). The methods for quantitation of hydrastine in both serum and urine were developed and validated in our laboratory (Gupta et al., 2009). Briefly, serum or urine samples were thawed and immediately processed for LC-MS/MS analysis. Sample preparation for LC-MS/MS analysis was performed by precipitation of serum proteins using four volumes of acetonitrile; noscapine served as the internal standard (IS). The supernatant obtained after centrifugation (10 min at room temperature, 7000 X g) was dried under nitrogen and the residue was reconstituted in 1 volume of methanol and 5 μ l was injected onto the LC-MS/MS system.

Urine samples were diluted 5X in control human serum and the sample preparation and LC-MS/MS conditions were identical to those described above for serum. Dilution of urine with serum afforded a matrix more similar to serum leading to fewer unexpected matrix ion effects.

Chemical stability of hydrastine: The stability of hydrastine in human serum and urine under sample handling conditions was determined. Control serum or urine was spiked at 1, 100 and 500 ng/ml hydrastine and then subjected to three-freeze thaw cycles. Hydrastine concentration was determined after each freeze-thaw cycle.

LC/Q-ToF MS conditions: The LC-MS analysis of hydrastine phase I and phase II metabolites in human serum and urine was performed using a LC system consisting of a SIL-HTa autosampler coupled to two Shimadzu 10ADvp pumps (Shimadzu Corp.,

DMD #59410

Columbia, MD). The MS system was a Q-ToF Micro (Waters Corp., Milford, MA).

Instrument control and data acquisition was accomplished using MassLynx 4.1.

Chromatographic separation was achieved on a Phenyl-hexyl HPLC column, 100 mm × 2.1 (i.d.) mm, 3 μm, (Thermo Fisher Scientific, Waltham, MA) with a gradient system consisting of 20 mM ammonium formate, pH 2.7 (A), and 95% acetonitrile containing 20 mM ammonium formate, pH 2.7 (B) at a flow rate of 0.4 mL/min. The initial mobile phase condition was 5 % B which was increased linearly to 35 % B over 40 min, then increased to 90% B over 1 min and held for 4 min. The mobile phase conditions were returned to the initial conditions and held there for 4 min. The total chromatographic run time was 50 min.

Mass spectrometry was performed in positive ionization mode with an electrospray ionization source (ESI) interface. The capillary voltage was set to 2500 V, and the cone voltage was 25 V. The desolvation and cone gas flow rates were 600 L/h and 50 L/h, respectively. The source temperature was 150 °C, and the dissolution temperature was 400 °C. The mass analyzer was calibrated using 10 mM sodium formate.

Characterization of phase I and phase II metabolites of hydrastine using Liquid

Chromatography-High resolution mass spectrometry (LC-HRMS): The

characterization of hydrastine phase I and phase II metabolites in human serum and urine was performed using a LC system consisting of a SIL-HTa autosampler coupled to two Shimadzu 10ADvp pumps (Shimadzu Corp., Columbia, MD). The MS system was a Q-ToF Micro (Waters Corp., Milford, MA). Instrument control and data acquisition were accomplished using MassLynx 4.1. The mass spectrometer was calibrated by using a

DMD #59410

200 mM solution of sodium formate in 90% isopropanol in positive ion mode. The peak m/z 566.8892 in the sodium formate calibration solution mass spectrum was used as lock mass for accurate mass measurement.

Different mass spectrometric data acquisition and data mining techniques based on high resolution and accurate mass measurement capabilities of the Q-ToF instrument were used to characterize proposed metabolites of hydrastine.

Accurate mass of hydrastine metabolites: The MS data acquisition in the range m/z 100-1000 was performed at low collision energy (5 eV) to acquire mass spectra corresponding of intact hydrastine metabolites (MS scan). Expected hydrastine metabolites, based on the current understanding of metabolic pathways, were located by extracted ion chromatogram data corresponding to protonated ions of these metabolites. Spectra corresponding to each chromatographic peak (greater than 5% intensity of hydrastine peak area) were extracted from a single scan in the middle of the peak. Each extracted spectrum was searched for expected phase I and phase II metabolites of hydrastine, and the mass peak(s) matching with the accurate mass of expected phase I and phase II metabolites of hydrastine were located. Expected metabolites were predicted based on common metabolic reactions (i.e., demethylation, hydroxylation, hydrolysis, etc.). The elemental composition of identified metabolites was determined by using the built-in elemental composition determination tool of MassLynx, which uses accurate mass and isotope composition of ions to arrive at possible elemental formulae. The accurate mass match cut-off for elemental composition determination of putative metabolites was set at $\Delta = 5$ ppm for all analyses performed in this study.

DMD #59410

Pseudo-product ion scan: Another MS acquisition was performed in the same m/z range using intermediate collision energy of 15 eV, which resulted in non-selective in-source fragmentation of ions entering the mass analyzer. Mass spectra corresponding to each chromatographic peak contained the precursor ion as well as the product ions (pseudo-product ion scan). Data mining for hydrastine metabolites was performed using extracted ion chromatograms of characteristic fragment ions for hydrastine (m/z 176, m/z 178, m/z 188, m/z 190 and m/z 192) after phase I metabolism. Production of these product ions could be reasoned from fragmentation of the tetrahydro isoquinoline group.

Data Dependent Acquisition (DDA): Characteristic neutral loss from phase II metabolites (m/z 42 for acetyl, m/z 80 for sulfates, m/z 120 for cysteine conjugates, m/z 129 for glutathione conjugates, m/z 162 for mercapturic acid, and m/z 176 for glucuronides) was used to identify additional metabolites. The mass spectrometer was operated in DDA mode and parent ions exhibiting characteristic neutral losses were acquired automatically. Each peak selected on the basis of a neutral loss was subjected to collision-induced dissociation (CID) to obtain further fragmentation. The peaks exhibiting the neutral losses corresponding to phase II metabolites and also the fragmentation ions characteristic of hydrastine and its expected phase I metabolites were identified manually. The DDA mode was also used to obtain detailed fragmentation patterns of various phase I and phase II metabolites of hydrastine in separate runs. CID was triggered for the ions present in a list. For structural characterization of phase I metabolites, the list consisted of phase I metabolites, and the mass spectrometer was operated at low collision energy (5 eV) for selection of ions. For structural characterization of phase II metabolites the list again consisted of the

DMD #59410

corresponding phase I metabolites but the mass spectrometer was operated at intermediate collision energy of 15 eV. This is because CID of phase II metabolites leads to the neutral loss of phase II conjugate, and very little structural information is obtained.

Chromatographic retention time as well as MS/MS fragmentation characteristic of each identified metabolite was used for structure assignment. The MS scan was performed with Q-ToF Micro operating at intermediate collision energy (15 eV), resulting in some non-selective fragmentation of positively charged ions entering the collision cell. The extracted ion chromatograms were generated for m/z 190, 176, 178 and 188.

Metabolynx software: In another approach, Waters Metabolynx software was used to search for various expected and unexpected metabolites of hydrastine. Mass chromatograms and mass spectral data were acquired by MassLynx software in continuum format and were further processed by MetaboLynx software to screen and identify potential hydrastine metabolites through the mass difference from positively charged hydrastine ion (m/z , 384.1447), based on known metabolic pathways.

Profiling of exogenous goldenseal metabolites: Goldenseal powder (2 g) from Nature's Resource capsule was added to 10 mL of methanol and sonicated for 5 min then mixed for 4 h on an orbital shaker. The mixture was then centrifuged for 5 min at 6000 rcf and the supernatant was collected. The supernatant was diluted 45,000-fold in methanol and analyzed by LC-QToF MS. Analysis was performed by directly infusing the diluted supernatant into the mass spectrometer at a flow rate of 10 μ L/min. The diluent consisted of 25% acetonitrile containing 20 mM ammonium formate (pH 2.7). The Q-ToF micro mass spectrometer was operated in positive ion Electrospray

DMD #59410

ionization (+ESI) mode. The data was acquired in centroid mode using sodium formate as lock mass (m/z 566.8892).

Glucuronidase/Sulfatase treatment of serum and urine samples: Glucuronide conjugates of hydrastine phase I metabolites present in serum or urine diluted 5X in control human serum were hydrolyzed to the corresponding phase I metabolites in the presence of 125 mM citrate-phosphate buffer (pH 3.8) and 9 U/ μ L glucuronidase at 45 °C for 4 h. The combination of phosphate ions and pH 3.8 inhibited sulfatase activity of the β -glucuronidase to a large extent. The optimal pH for sulfatase activity of *Helix pomatia* enzyme preparation has previously described and found to be 5.2 (Dodgson and Powell, 1959). The hydrolysis of sulfate conjugates of hydrastine phase I metabolites was performed by incubating the serum or urine sample in the presence of 100 mM Tris-acetate buffer, pH 6.6 and 0.5 U/ μ L sulfatase at 45 °C for 24 h.

Hydrastine pharmacokinetics: Serum concentration-versus-time profiles for hydrastine were constructed and the pharmacokinetic parameters determined by non-compartmental analysis using PK-Solutions Version 2.0 (Summit Research Services; Montrose, CO).

DMD #59410

RESULTS

Both expected and unexpected metabolites of hydrastine were characterized using a high resolution LC-MS set up (LC-QToF) and various data acquisition and data mining techniques. No study subjects reported any adverse events within seven days of goldenseal consumption.

Method validation.

Extraction recovery of hydrastine from serum was 90.6%. The lower limit of quantitation for hydrastine in human serum was 0.1 ng/mL. The method was selective, linear (0.1 - 1000 ng/mL), accurate (predicted values 80 - 120% of actual), and precise (CV<15%). The method was rugged with respect to the absence inter-subject variability of the analytical response and the stability of the analytes.

Extraction recovery of hydrastine from urine was 85.0%. The lower limit of quantitation for hydrastine in urine was 1 ng/mL. The method was selective, linear (1 - 1000 ng/mL) accurate (predicted values 80 - 120% of actual), and precise (CV<15%). The method was reliable with respect to the absence inter-subject variability of the analytical response and stability of analytes.

Chemical stability of hydrastine: Hydrastine was found to be stable under the sample handling conditions. There was no significant reduction in hydrastine concentrations in the spiked serum and urine samples tested under three different conditions. The prepared samples were also found to be stable under the autosampler conditions (25 °C) for at least 60 h (data not shown).

DMD #59410

Profiling of endogenous goldenseal components: It was important to confirm that metabolites related to hydrastine found in human biologic matrices were not endogenously present in goldenseal supplement. The mass spectrum obtained from the direct infusion of diluted goldenseal extract into the mass spectrometer was searched for hydrastine metabolites identified in serum and urine of human subjects. The identified hydrastine metabolites were also searched in the LC-MS chromatogram of diluted goldenseal extract, extracting ion chromatograms corresponding to m/z of identified metabolites. None of the hydrastine metabolites identified in human urine and serum were found to be endogenously present in the goldenseal supplement. The alkaloids hydrastine and berberine were found to be major components of goldenseal, whereas canadine and canadine were only present as minor components (Figure 1).

Interestingly, neither hydrastidine (m/z 370) nor isohydrastidine (m/z 370) was detected in the goldenseal extract though others have reported finding this compound in *Hydrastis canadensis* (Messana et al., 1980; Le et al., 2014). Both hydrastidine and isohydrastidine share the same elemental composition (i.e., $C_{20}H_{20}NO_6^+$) and therefore share the same m/z -value of 370.1212. Canadine ($C_{21}H_{24}NO_5^+$ m/z 370.1654), which was found in the goldenseal extract, does not share the same elemental composition or exact mass as the hydrastidine isomers. This difference is due to the mass defect associated with excess oxygen, which has a lower mass relative to carbon, nitrogen and hydrogen, in canadine. Metabolites M18 and M19 are possible phase II metabolites of hydrastidine or isohydrastidine or as we propose here, hydrastidine and/or isohydrastidine are in vivo metabolites formed from the *O*-demethylation of hydrastine. The logic behind this proposed pathway rests with the fact that neither hydrastidine nor

DMD #59410

isohydrastidine was detected in the Goldenseal material used for this study. But this proposed pathway is offered with some caution because of the chemical complexity of Hydrastis or any other natural product, the phytochemical profile shown here is certainly not comprehensive and the source of hydrastidine and isohydrastidine may originate from the plant and not human metabolism.

Hydrastine Pharmacokinetics. Figure 2 indicates that hydrastine was rapidly absorbed. Additionally, the bioavailability of hydrastine, relative that reported elsewhere for berberine was significant. (Gupta et al., 2009; Godugu et al., 2014) Pharmacokinetic parameters for Hydrastine are shown in Table 1. Very little hydrastine (0.16%) was excreted unchanged in the urine, suggesting significant pre-systemic metabolism, or distribution into other tissues. Since the oral bioavailability is unknown, the apparent volume of distribution cannot be determined from these data. The high degree of variability in C_{max} suggests that the pharmacological response associated with hydrastine might also be variable.

Very little has been reported on the pharmacological activity of (-)(1S,9R)- β -hydrastine. Abdel-haq *et. al.* have shown that ethanolic extracts of *Hydrastis* increased cyclic AMP levels and induced relaxation in carbachol-precontracted isolated trachea (Abdel-Haq et al., 2000). The relaxant effect had an EC_{50} of 1.5 μ g/ml and 73 μ g/ml for *Hydrastis* extract and hydrastine, respectively. The authors concluded that hydrastine and the other key isoquinoline alkaloids, berberine, canadine, and canadoline were responsible for the relaxant effects of *Hydrastis by acting at adrenergic and adenosinic receptors*. The relaxant effects of canadoline and hydrastine were inhibited by xanthine

DMD #59410

amine congener, while timolol inhibited the relaxant effects of canadine and canadoline but not that of berberine or hydrastine. (Abdel-Haq et al., 2000) These in vitro data suggest that hydrastine concentrations never reach therapeutic levels, at least within the framework of increases in cyclic AMP. But due to the chemical complexity of the *Hydrastis* extract, it is very difficult to make any correlations between the serum levels reported herein and a pharmacodynamic response related to *Hydrastis* consumption.

CID spectrum of hydrastine. The MS/MS fragmentation pattern of hydrastine used for identification and structural assignment of phase I and phase II metabolites of hydrastine is shown in Figure 3. The hydrastine molecule can be visualized as two chemical moieties, the isoquinoline ring system and the phthalide ring system, which are of similar molecular masses connected by a single C-C bond between carbon 1 and carbon 9. In collision-induced dissociation (CID) this C1-C9 bond is easily cleaved and a major charged fragment at m/z 190 (corresponding to the isoquinoline group) is observed following the neutral loss of the phthalide (Figure 3). This fragmentation pattern was also expected for a number of phase I and phase II metabolites of hydrastine and was used for ‘fishing’ of various phase I and phase II metabolites of hydrastine. The relationship between the hydrastine metabolites thus found and the ‘fishing line’ fragment initially used to localize this metabolite was confirmed by exact superimposition of the LC-MS peaks of the two ions in the extracted ion chromatograms. Table 2 shows proposed structures for of each diagnostic product ion observed for hydrastine and metabolites. Metabolites associated with the observed product ion are indicated in Table 2 by their assigned abbreviation.

Metabolites which did not exhibit the characteristic CID fragmentation as described above were searched in the spectra corresponding to the chromatographic peaks in the extracted ion chromatogram of nominal m/z of these metabolites and then determined by matching the accurate mass.

Hydrastine metabolism. Retention times (t_R), exact mass, and proposed structures for hydrastine, various hydrastine phase I metabolites, and phase II metabolites are given in Table 3. Ambiguities in structures are indicated with a dotted oval to indicate potential position of functional groups. Total Ion Chromatograms (TIC) and Base Peak Intensity (BPI) chromatograms of pre-dose and post-dose urine samples were compared to identify metabolite peaks. However, due to the low dose of Goldenseal supplement (in the range normally used for therapeutic intervention) and extensive interference from serum and urine matrix components, no useful information could be obtained from comparing the total ion current (TIC) of the pre-dose and post-dose urine samples. Extracted ion chromatograms are shown in Figure 4 and grouped according to peak area relative to hydrastine, for clarity. The peaks areas reported in Table 2 are the average values obtained from the eleven subjects who completed the study.

The largest peak (M5) was detected at m/z 188.0712 and a retention time of 15.6 min. This compound was tentatively identified as 6-methyl-1,3-dioxolo[4,5-g]isoquinolinium, (i.e., hydrastonine). Preliminary results on pharmacology of this metabolite and evidence for its presence in the bark of *Cryptocarya chinensis* have been reported by Lin *et al* (Lin *et al.*, 2002). Structurally, M5 is similar to the neurotoxin 1-methyl-4-phenyl-1,2,3,6-tetrahydropyridine (MPTP), which may have some bearing on the safety

DMD #59410

of *Hydrastis*. In addition, four reports have addressed the potential toxicity of methylenedioxy-*N*-methyloquinoline, which may translate to possible untoward effects of M5 on mitochondrial respiration (McNaught et al., 1996a), dopamine reuptake (McNaught et al., 1996b), and nigral cell viability (McNaught et al., 1996c). These concerns, however, are relevant only if M5 is formed in the brain from the reduced precursor, which was not detected in urine or serum. Moreover, M5 is a quaternary ammonium compound and is unlikely to cross the blood brain barrier.

Table 5 provides area under the peak area time curve and elimination half-lives for the three major hydrastine metabolites detected in serum of all subjects and hydrastine. These metabolites included M1 (hydrohydrastinin), M36, and M41. Data for hydrastine was also determined here using the integrated chromatographic peak area for hydrastine to enable a quasi-direct comparison to the metabolites listed in Table 5. A direct comparison was not feasible here since the ionization efficiency for the metabolites relative to hydrastine could not be determined. But based on this quasi-comparison, the bioavailable for these three metabolites was comparable to that observed for hydrastine. Ten unique metabolites were detected in two or more subjects completing the study. Three of these proposed hydrastine metabolites were detected in all eleven subjects (M1, M36, and M41). M36 was consistently detected in serum with an apparent elimination half-life of 5 hours. The mass-to-charge and mass fragmentation pattern for M36 was consistent with hydrolysis of the lactone ring of the phthalide group. The fragmentation pattern for M41 was consistent with neutral loss of 176 (glucuronide) and a fragment ion observed at m/z 192. Peaks corresponding to these retention times or mass-to-charge ratios were not observed in the pre-dose serum

DMD #59410

samples for any of the subjects. The presence of several other hydrastine metabolites was also detected in the serum of some of the 11 subjects participating in the study.

M33 (m/z 548) was detected in 8 of the 11 subjects with an elimination half-life of 3.5 ± 1.5 hours. Other metabolites were detected in less than half the subjects and chromatographic peak areas were not sufficient to estimate an elimination half-life.

The principal phase I metabolite of hydrastine (M40) was observed at m/z = 386.1605 with a retention time of 25.8 min, and a peak area representing 62% of the area obtained for hydrastine. The putative phase II metabolite of M40 was observed at 18.4 min with m/z 562.1921 and a peak area representing 309% of the peak area obtained for hydrastine. This peak M41 in Table 3 showed the largest LC-ToF peak area compared with hydrastine and other hydrastine metabolites. Other major metabolites were represented by four peaks with an m/z of 548 (t_r = 12.8 min, M21; t_r = 13.0 min, M22; t_r =16.7 min, M32; t_r =17.3 min, M33). A proposed reaction pathway for the metabolism of hydrastine is shown in Figure 5a and Figure 5b. The authenticity of phase II metabolites was corroborated by the fact that chromatographic peaks assigned to the glucuronides were not detected after treatment with β -glucuronidase. These observations suggest that hydrastine is metabolized *via* phase I and phase II pathways, a finding not uncommon for plant secondary metabolites consumed by humans. High resolution mass spectrometry of the goldenseal extract confirmed that these compounds were not present in goldenseal prior to administration. Using hydrastine as a surrogate calibration standard, the concentrations of hydrastine metabolites excreted in the urine were estimated. Using this approach, approximately 30% of the absorbed hydrastine dose was excreted in urine as metabolites. While the remaining 70% may

DMD #59410

undergo biliary excretion, it is also possible that hydrastine has a large distribution volume and is largely disseminated into peripheral tissues where they may elicit a therapeutic response. Tentative assignment of specific enzymes responsible for each reaction is provided when feasible. These assignments were made based on thorough studies of the metabolism of noscapine, a structural analogue of hydrastine, but not present in goldenseal. (Tsunoda and Yoshimura, 1979; Tsunoda and Yoshimura, 1981; Fang et al., 2012)

A limitation of this study was the fact that goldenseal is a complex mixture of component, many of which are similar in mass to that of hydrastine and the metabolites reported here. This of course means that we cannot conclusively say that the compounds characterized here are indeed associated with hydrastine metabolism. Nor can conclusive structures be assigned using mass spectral data alone. But these studies do show the potential importance of hydrastine and should encourage an increase in the study of hydrastine metabolism and pharmacological activity.

Canadaline Metabolism. While an investigation of hydrastine deposition was the primary aim of the work presented herein, we discovered significant absorption and metabolism of a related alkaloid, canadaline. The m/z of 370 assigned to this component was similar to hydrastine metabolites and for this reason we have included its description here. Canadaline, a secoberbine alkaloid, is of particular interest because it contains a potentially reactive aldehyde. Table 4 shows LC-ESI-ToF data for proposed canadaline metabolites. Fifteen isoquinoline alkaloids, including canadaline, were recently isolated from *Corydalis cava* and subsequently tested for human blood acetylcholinesterase (AChE) and human plasma butyrylcholinesterase (BuChE)

DMD #59410

inhibitory activity (Chlebek et al., 2011). Canadoline reportedly had IC₅₀ values of 20 μ M and 85 μ M for AChE, and BuChE, respectively. Chlebek et al. also isolated (+)-canadine, and reported an IC₅₀ value of 12.4 μ M for AChE. These anti-cholinesterase properties of isoquinoline alkaloids might contribute to the anti-diarrheal effects of goldenseal.

DMD #59410

DISCUSSION

The discovery of new drugs from natural products has been a goal of pharmacognosy for nearly two centuries. Given the large number of hydrastine metabolites reported herein, it is possible that one of these metabolites may have positive pharmacologic effects and pursuing further study of the structural and pharmacological activity of these compounds is important. Much of what is known about the metabolic fate and disposition of phytochemicals has been studied within the context of functional foods and herbal products. The term metabolic activation describes the various metabolic mechanisms responsible for the conversion of small molecules found in plants into metabolites that invoke either a therapeutic or toxic response in humans or other mammals (Chen et al., 2011). Due in part to prevalence of flavonoids in food and dietary supplements, flavonoids have received significant attention in the literature for their potential therapeutic properties. This is reflected in 2381 review articles indexed by Pubmed. Recent reviews on the subject have highlighted the potential importance of flavonoid phase II metabolites (Zhang et al., 2007; Perez-Vizcaino et al., 2012), since the apparent exposure to the aglycone is small in comparison to the conjugated glucuronide form. Perez-Vizcaino, *et al.*, have suggested that flavonoid glucuronides are hydrolyzed in the cell membrane, and the active aglycones are released in the cell (Perez-Vizcaino et al., 2012). This mechanism was used to explain the paradox that flavonoids appear to have biological activity despite having low bioavailability. Phase II metabolites, can also evoke toxicity in the presence of sulfotransferase activity and one of several functional groups that may include benzylic and allylic alcohols, aromatic hydroxylamines, and hydroxamic acids (Banoglu, 2000; Yi et al., 2006).

DMD #59410

This is the first comprehensive description of hydrastine disposition in humans following ingestion of a standardized goldenseal extract. This study has shown that hydrastine is extensively metabolized by both phase I and phase II reactions. The implication of these observations is the possibility that any pharmacological response from ingestion of goldenseal may be due to active metabolites of hydrastine. This then invokes the possibility that the therapeutic response to berberine, hydrastine or goldenseal supplement would be variable and dependent the drug metabolizing enzyme phenotype of individuals. The goldenseal dose chosen for this study was based on large part on the daily dose recommended by the manufacturer, but it was also chosen because this dose was used in previous herb-drug-interaction studies conducted by our group.(Gurley et al., 2008b) Because the dose in the present study and in earlier studies where clinically significant effects of goldenseal were observed, it can easily be reasoned that the parent compound (hydrastine) or its metabolites are responsible for the effects observed earlier. In our earlier herb-drug-interaction study, subjects consumed 1.07 g of goldenseal three times daily (morning, noon, and evening) for two weeks and then were phenotyped for CYP2D6 and CYP3A4 activity. This dosing within a 12-hour period was approximately equal to the elimination half-life for hydrastine ($t_{1/2}$ = 4.8 h; Table 1). Goldenseal was not taken during the night, so there was likely time for hydrastine to wash out, though this would have to be confirmed with actual pharmacokinetic studies with the dosing regimen. But certainly the three metabolites listed in Table 5 (M1, M36, and M41) with elimination half-lives comparable or longer than hydrastine (i.e., ≥ 5 h) might be better candidates for eliciting the observed effect on CYP2D6 and CYP3A4 activity. In fact, these metabolites might achieve steady-state

DMD #59410

concentration following daily consumption of goldenseal for two weeks. In the present study a single dose of goldenseal containing 78 mg of hydrastine, was administered in order to determine baseline pharmacokinetic parameters and in order to fully understand the pharmacokinetic implications of goldenseal affects, the pharmacokinetics should be determined at the beginning of and end of a multiple dose regimen. While berberine, hydrastine, and canadine pharmacology has been reported, the pharmacological action of other phytochemicals present in *Hydrastis canadensis* remains a relatively unexplored area. The action of these other phytochemicals, particularly isohydrastidine (M19 or M18 phase II metabolite), should be explored given the data presented here.

The examples highlighted above suggest that phase II metabolites of hydrastine may also have biological activity or that these conjugated metabolites may be important intermediates in the transport of hydrastine phase I metabolites to their cellular receptors. It cannot be overstated though that a full evaluation of the chemical structure was not done for metabolites proposed here. Further characterization by NMR spectroscopy is critical to a full elucidation of the structure for the compounds proposed here. But given strong evidence suggested by LC-MS data for the formation of potentially active hydrastine metabolites, more efforts to study the therapeutic potential of these compounds is warranted.

DMD #59410

Acknowledgments.

Authorship Contributions:

Participated in research design: Hendrickson, Gurley, Barone

Conducted experiments: Gupta, Hendrickson

Performed data analysis: Gupta, Hendrickson, Fifer

Wrote or contributed to writing of the manuscript: Gupta, Hendrickson, Gurley, Fifer

DMD #59410

References

- Abdel-Haq H, Cometa MF, Palmery M, Leone MG, Silvestrini B, and Saso L (2000) Relaxant effects of *Hydrastis canadensis* L. and its major alkaloids on guinea pig isolated trachea. *Pharmacol Toxicol (Copenhagen)* **87**:218-222.
- Abourashed EA and Khan IA (2001) High-performance liquid chromatography determination of hydrastine and berberine in dietary supplements containing goldenseal. *Journal of pharmaceutical sciences* **90**:817-822.
- Banoglu E (2000) Current status of the cytosolic sulfotransferases in the metabolic activation of promutagens and procarcinogens. *Current drug metabolism* **1**:1-30.
- Blaskó G, Gula DJ, and Shamma M (1982) The Phthalideisoquinoline Alkaloids. *Journal of Natural Products* **45**:105-122.
- Blumenthal M, Brinckmann J, and Wollschlaeger B (2003) *The ABC clinical guide to herbs*. American Botanical Council, Austin, Tex.
- Chatterjee P and Franklin MR (2003) Human cytochrome P450 inhibition and metabolic-intermediate complex formation by goldenseal extract and its methylenedioxyphenyl components. *Drug Metab Dispos* **31**:1391-1397.
- Chen JL, Zhang YL, Dong Y, Gong JY, and Cui HM (2013) [CYP450 enzyme inhibition of berberine in pooled human liver microsomes by cocktail probe drugs]. *Zhongguo Zhong Yao Za Zhi* **38**:2009-2014.

DMD #59410

Chen XW, Serag ES, Sneed KB, and Zhou SF (2011) Herbal bioactivation, molecular targets and the toxicity relevance. *Chem Biol Interact* **192**:161-176.

Chlebek J, Macakova K, Cahlikovi L, Kurfurst M, Kunes J, and Opletal L (2011) Acetylcholinesterase and butyrylcholinesterase inhibitory compounds from *Corydalis cava* (Fumariaceae). *Natural product communications* **6**:607-610.

Dodgson KS and Powell GM (1959) Studies on sulphatases. 26. Arylsulphatase activity in the digestive juice and digestive gland of *Helix pomatia*. *Biochemical Journal* **73**:666-671.

Dunnick JK, Singh B, Nyska A, Peckham J, Kissling GE, and Sanders JM (2011) Investigating the potential for toxicity from long-term use of the herbal products, goldenseal and milk thistle. *Toxicol Pathol* **39**:398-409.

Etheridge AS, Black SR, Patel PR, So J, and Mathews JM (2007) An in vitro evaluation of cytochrome P450 inhibition and P-glycoprotein interaction with goldenseal, Ginkgo biloba, grape seed, milk thistle, and ginseng extracts and their constituents. *Planta Med* **73**:731-741.

Fang ZZ, Krausz KW, Li F, Cheng J, Tanaka N, and Gonzalez FJ (2012) Metabolic map and bioactivation of the anti-tumour drug nescapine. *Br J Pharmacol* **167**:1271-1286.

Godugu C, Patel AR, Doddapaneni R, Somagoni J, and Singh M (2014) Approaches to improve the oral bioavailability and effects of novel anticancer drugs berberine and betulinic acid. *PLoS One* **9**:e89919.

DMD #59410

Gupta PK, Hubbard M, Gurley B, and Hendrickson HP (2009) Validation of a liquid chromatography-tandem mass spectrometric assay for the quantitative determination of hydrastine and berberine in human serum. *J Pharm Biomed Anal* **49**:1021-1026.

Gurley BJ, Swain A, Barone GW, Williams DK, Breen P, Yates CR, Stuart LB, Hubbard MA, Tong Y, and Cheboyina S (2007) Effect of goldenseal (*Hydrastis canadensis*) and kava kava (*Piper methysticum*) supplementation on digoxin pharmacokinetics in humans. *Drug Metab Dispos* **35**:240-245.

Gurley BJ, Swain A, Hubbard MA, Hartsfield F, Thaden J, Williams DK, Gentry WB, and Tong Y (2008a) Supplementation with goldenseal (*Hydrastis canadensis*), but not kava kava (*Piper methysticum*), inhibits human CYP3A activity in vivo. *Clinical Pharmacology and Therapeutics* **83**:61-69.

Gurley BJ, Swain A, Hubbard MA, Williams DK, Barone G, Hartsfield F, Tong Y, Carrier DJ, Cheboyina S, and Battu SK (2008b) Clinical assessment of CYP2D6-mediated herb-drug interactions in humans: effects of milk thistle, black cohosh, goldenseal, kava kava, St. John's wort, and Echinacea. *Mol Nutr Food Res* **52**:755-763.

Le PM, McCooeye M, and Windust A (2014) Application of UPLC-QTOF-MS in MS(E) mode for the rapid and precise identification of alkaloids in goldenseal (*Hydrastis canadensis*). *Anal Bioanal Chem* **406**:1739-1749.

Lin FW, Wang JJ, and Wu TS (2002) New pavine N-oxide alkaloids from the stem bark of *Cryptocarya chinensis* Hemsl. *Chem Pharm Bull (Tokyo)* **50**:157-159.

DMD #59410

McNaught KS, Thull U, Carrupt PA, Altomare C, Cellamare S, Carotti A, Testa B, Jenner P, and Marsden CD (1996a) Effects of isoquinoline derivatives structurally related to 1-methyl-4-phenyl-1,2,3,6-tetrahydropyridine (MPTP) on mitochondrial respiration. *Biochem Pharmacol* **51**:1503-1511.

McNaught KS, Thull U, Carrupt PA, Altomare C, Cellamare S, Carotti A, Testa B, Jenner P, and Marsden CD (1996b) Inhibition of [3H]dopamine uptake into striatal synaptosomes by isoquinoline derivatives structurally related to 1-methyl-4-phenyl-1,2,3,6-tetrahydropyridine. *Biochem Pharmacol* **52**:29-34.

McNaught KS, Thull U, Carrupt PA, Altomare C, Cellamare S, Carotti A, Testa B, Jenner P, and Marsden CD (1996c) Nigral cell loss produced by infusion of isoquinoline derivatives structurally related to 1-methyl-4-phenyl-1,2,3,6-tetrahydropyridine. *Neurodegeneration* **5**:265-274.

Messana I, La BR, and Galeffi C (1980) The alkaloids of *Hydrastis canadensis* L. (Ranunculaceae). Two new alkaloids: hydrastidine and isohydrastidine. *Gazz Chim Ital* **110**:539-543.

Perez-Vizcaino F, Duarte J, and Santos-Buelga C (2012) The flavonoid paradox: conjugation and deconjugation as key steps for the biological activity of flavonoids. *Journal of the science of food and agriculture* **92**:1822-1825.

Raner GM, Cornelious S, Moulick K, Wang Y, Mortenson A, and Cech NB (2007) Effects of herbal products and their constituents on human cytochrome P450E1 activity. *Food Chem Toxicol* **45**:2359-2365.

DMD #59410

Tsunoda N and Yoshimura H (1979) Metabolic fate of noscapine. II. Isolation and identification of novel metabolites produced by carbon-carbon bond cleavage. *Xenobiotica* **9**:181-187.

Tsunoda N and Yoshimura H (1981) Metabolic fate of noscapine. III. Further studies on identification and determination of the metabolites. *Xenobiotica* **11**:23-32.

Weber HA, Zart MK, Hodges AE, Molloy HM, O'Brien BM, Moody LA, Clark AP, Harris RK, Overstreet JD, and Smith CS (2003) Chemical comparison of goldenseal (*Hydrastis canadensis* L.) root powder from three commercial suppliers. *J Agric Food Chem* **51**:7352-7358.

Yi L, Dratter J, Wang C, Tunge JA, and Desaire H (2006) Identification of sulfation sites of metabolites and prediction of the compounds' biological effects. *Anal Bioanal Chem* **386**:666-674.

Yin SY, Lee JJ, Kim YM, Jin CM, Yang YJ, Kang MH, Kai M, and Lee MK (2004) Effects of (1R,9S)- β -hydrastine on L-DOPA-induced cytotoxicity in PC12 cells. *Eur J Pharmacol* **488**:71-77.

Zhang L, Zuo Z, and Lin G (2007) Intestinal and hepatic glucuronidation of flavonoids. *Molecular pharmaceutics* **4**:833-845.

DMD #59410

Legends for Figures

Figure 1. Analysis of chemical constituents of goldenseal supplement. A) Mass spectrum of goldenseal extract diluted in methanol containing 0.1% formic acid. Diluted extract was directly infused into the electrospray source and mass analyzer at a flow rate of 10 μ L/min. The inset shows the area of spectrum from m/z 325 to m/z 400. Peaks (m/z) corresponding to berberine, canadine, berberastine, canadine, and hydrastine are numbered 1, 2, 3, 4, and 5, respectively. B) Extracted ion chromatograms (m/z 336, 340, 352, 370, and 384) from injection of diluted goldenseal extract. Ion chromatograms were chosen based on the expected m/z for berberine, canadine, berberastine, canadine, and hydrastine.

Figure 2. Serum concentration time profile for hydrastine following administration of 2.7 g of goldenseal extract (containing 78 mg hydrastine) to healthy human volunteers. Circles are the Mean \pm SEM (n=11). The solid line was generated using a noncompartmental technique based on the method of residuals.

Figure 3. Characteristic fragmentation pathway used in structure assignment of hydrastine metabolites. The mass spectrum was extracted from the chromatographic peak for hydrastine. Ionization was achieved using an electrospray interface operated in positive ion mode.

Figure 4. Typical LC-TOFMS chromatograms of urine following goldenseal consumption. Figures A-E represent unique extracted ion chromatograms from the same injection of urine. Proposed structure assignments for each peak are shown in Table 2.

Figure 5. Proposed phase I and phase II metabolism of hydrastine. Specific enzymes are provided when possible and assignment of these enzymes was made based on known metabolic reactions

DMD #59410

for noscapine a naturally occurring structural analogue of hydrastine. CYP = cytochrome P450,
MAO = monoamine oxidase, PON1 = Human serum paraoxonase,

DMD #59410

Table 1

Pharmacokinetic parameters for hydrastine.

Values are the Mean \pm Standard Deviation (n=11)

Dose (mg/kg)	t _{max} (h)	C _{max} (ng/mL)	AUC (ng-h/mL)	t _{1/2} (h)	%Dose Excreted in Urine
1.13 \pm 0.31	1.2 \pm 0.3	208 \pm 126	495 \pm 217	4.8 \pm 1.4	0.16 \pm 0.14

DMD #59410

Table 2

Exact mass and structure for diagnostic product ions observed in tandem mass spectrum analysis
of Hydrastine metabolites.

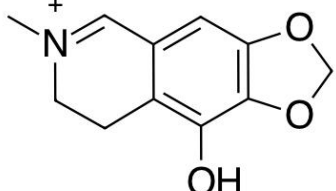
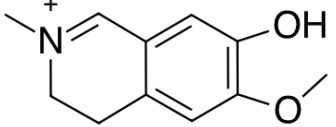
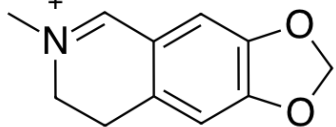
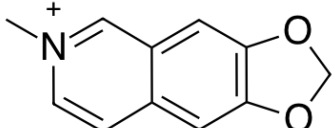
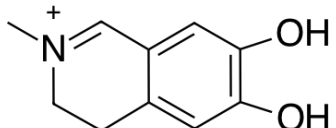
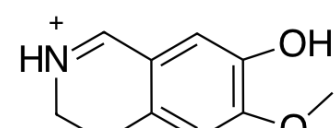
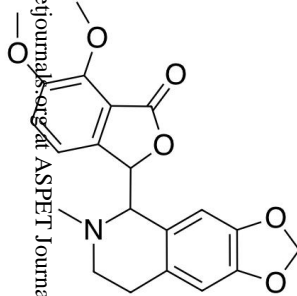
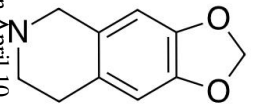
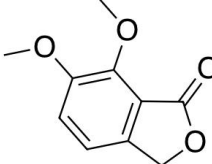
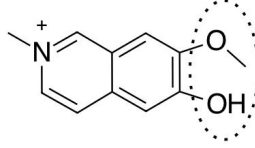
<i>m/z</i>	Metabolites with this product ion	Structure of product ion
206.0812	M39	
192.1019	M20, M21, M37, M40, M41	
190.0863	Hydrastine, M11, M12, M15, M18, M19	
188.0706	M10, M13, M14	
178.0863	M16, M27, M29, M30, M32, M33,	
176.0706	M25, M34	

Table 3

Chromatographic and ESI-TOF data of hydrastine and proposed metabolites in urine from healthy volunteers following oral administration of 2.7 g of goldenseal supplement (equivalent to 78 mg hydrastine).

ID	Proposed Reaction	t _R (min)	Expected ion (m/z)	Measured ion (m/z)	Formula	Peak area*	%Hydrastine	MS/MS fragments (m/z)	Proposed Structure
Hydrastine	Parent	37.3	384.1447	384.1430	C ₂₁ H ₂₀ NO ₆	625 ± 390	100	190.0892 293.0850 323.0825	
M1	C-C reduction	14.2	192.1024	192.1018 (+ 1.0)	C ₁₁ H ₁₃ NO ₂	261±135,	34	177.0787 162.0776	 Hydrohydrastinin
M2	C-C reduction	25.5	195.0657	195.0661 (2.0)	C ₁₀ H ₁₁ O ₄	45±19,	6	180.0443 162.0320	 Meconine
M3	C-C reduction, dehydrogenation/	15.4,	190.0868	190.0866 (-1.0),	C ₁₁ H ₁₂ NO ₂	1167±509	151	M3: 175.0633 147.0677 154.0508 132.0365	
M4	C-C reduction, C-O reduction, aromatization	15.8		190.0879 (+5.7)		778±312,	101	M4: 175.0626 160.0755 149.0581 132.0365	

Downloaded from https://pubs.aspetjournals.org/ at ASPET Journals on April 10, 2024

Table 3

Chromatographic and ESI-TOF data of hydrastine and proposed metabolites in urine from healthy volunteers following oral administration of 2.7 g of goldenseal supplement (equivalent to 78 mg hydrastine).

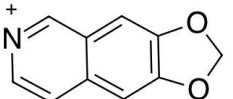
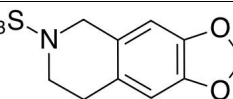
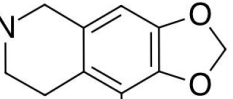
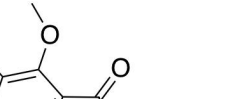
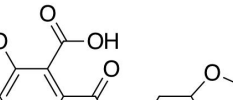
ID	Proposed Reaction	t _R (min)	Expected ion (m/z)	Measured ion (m/z)	Formula	Peak area*	%Hydrastine	MS/MS fragments (m/z)	Proposed Structure
M5	C-C reduction, aromatization	15.6	188.0712	188.0714 (+1.0)	C ₁₁ H ₁₀ NO ₂	3860±1442,	500	130.0555, 160.0676	 Hydrastinine
M7	C-C reduction, N-demethylation and N-sulfation	11.9	258.0436	258.0434 (-0.8)	C ₁₀ H ₁₂ NO ₆ S	137±72,	18	178.0868	 M7
M9	C-C reduction, N-demethylation, hydroxylation and O-glucuronidation	22.4	370.1138	370.1138 (0)	C ₁₆ H ₂₀ NO ₉	99±77,	13	194.0812	 M9
M10	C-C dehydrogenation	30.8	382.1291	382.1278 (-3.4)	C ₂₁ H ₂₀ NO ₆	74±42,	10	334.0744 322.1118 292.1011 278.0926 188.0712	 M10
M11	Lactone hydrolysis, alcohol dehydrogenation	27.6	400.1396	400.1388 (-2.0)	C ₂₁ H ₂₂ NO ₇	186±59,	24	382.1301 190.0866	 M11

Table 3

Chromatographic and ESI-TOF data of hydrastine and proposed metabolites in urine from healthy volunteers following oral administration of 2.7 g of goldenseal supplement (equivalent to 78 mg hydrastine).

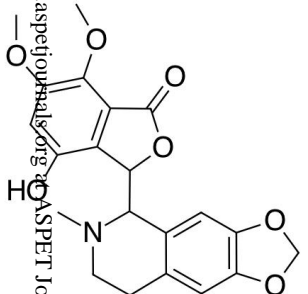
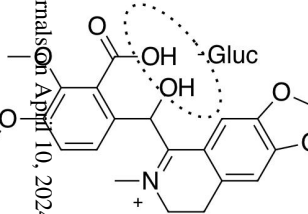
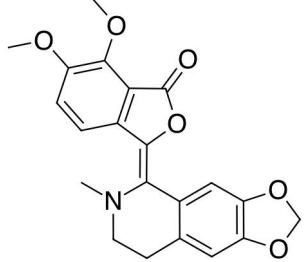
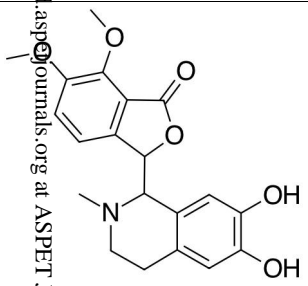
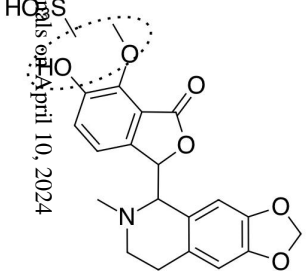
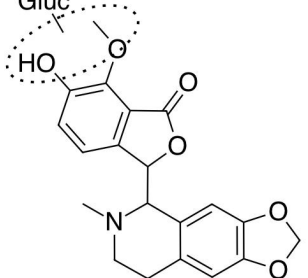
ID	Proposed Reaction	t _R (min)	Expected ion (m/z)	Measured ion (m/z)	Formula	Peak area*	%Hydrastine	MS/MS fragments (m/z)	Proposed Structure
M12	Hydroxylation	37.3	400.1396	400.1402	C ₂₁ H ₂₂ NO ₇ (+1.5)	304±157,	39	190.0866 311.0924 323.0917 335.0938 353.1053	
M13,14	Lactone hydrolysis, dehydrogenation, acyl glucuronidation	27.2, 28.8	576.1717	576.1706 (-1.9), 576.1705 (-2.1)	C ₂₇ H ₃₀ NO ₁₃	72±50,	9	M13: 382.1235 188.0721 M14: 382.1181 188.0697	
M15	C-C dehydrogenation	32.4	382.1291	382.1289 (-0.5)	C ₂₁ H ₂₀ NO ₆	154±98,	20	322.1089 307.1242 292.0983 278.0943 280.1007 190.0882	 CAS: 858196-25-5

Table 3

Chromatographic and ESI-TOF data of hydrastine and proposed metabolites in urine from healthy volunteers following oral administration of 2.7 g of goldenseal supplement (equivalent to 78 mg hydrastine).

ID	Proposed Reaction	t _R (min)	Expected ion (m/z)	Measured ion (m/z)	Formula	Peak area*	%Hydrastine	MS/MS fragments (m/z)	Proposed Structure
M16	C-O reduction, O-demethylation	21.4	372.1447	372.1437 (-2.7)	C ₂₀ H ₂₂ NO ₆	178±100,	23	354.1255 323.0909 311.0941 178.0859	 <p>CAS: 58298-46-7</p>
M18	O-demethylation, O-sulfation	27.4	450.0860	450.0851 (-1.8)	C ₂₀ H ₂₀ NO ₉ S	73±70,	9	370.1304 309.0805 190.0887	 <p>HO-S</p>
M19	O-demethylation, O-glucuronidation	19.9	546.1612	546.1607 (-0.9)	C ₂₆ H ₂₈ NO ₁₂	508±359,	66	370.1288 309.0797 190.0874	 <p>Gluc</p>

Downloaded from dmd.aspetjournals.org at ASPET Journals on April 10, 2024

Table 3

Chromatographic and ESI-TOF data of hydrastine and proposed metabolites in urine from healthy volunteers following oral administration of 2.7 g of goldenseal supplement (equivalent to 78 mg hydrastine).

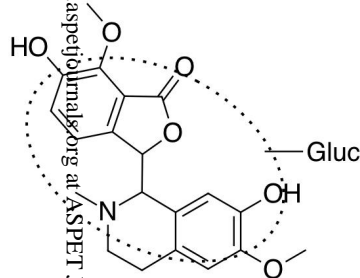
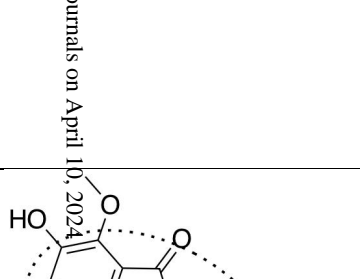
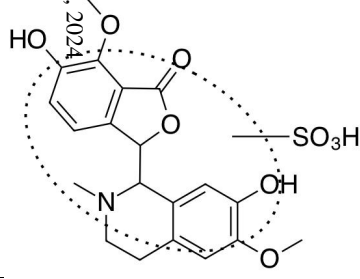
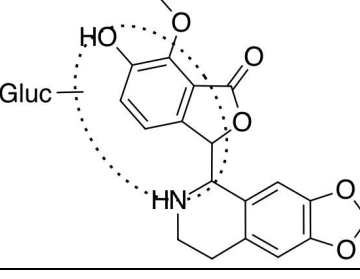
ID	Proposed Reaction	t _R (min)	Expected ion (m/z)	Measured ion (m/z)	Formula	Peak area*	%Hydrastine	MS/MS fragments (m/z)	Proposed Structure
M20	C-O reduction, O-demethylation, O-glucuronidation	12.1	548.1768	548.1740 (-5.1)	C ₂₆ H ₃₀ NO ₁₂	355±211,	46	372.1447 368.1266 311.0951 294.1451 192.1035	
M21	C-O reduction, O-demethylation, O-glucuronidation	12.5	548.1768	548.1758 (-1.8)	C ₂₆ H ₃₀ NO ₁₂	533±316,	69	372.1425 323.0960 311.0886 192.1035 165.0651 144.0820	
M22	C-O reduction, O-demethylation, O-sulfation	18.8	452.1016	452.1016 (0)	C ₂₀ H ₂₂ NO ₉ S	117±81,	15	372.1456 323.0952 311.0924 192.1018	
M25	N-demethylation, O-demethylation, O-glucuronidation	19.3	532.1455	532.1452 (-0.6)	C ₂₅ H ₂₆ NO ₁₂	220±138,	29	514.1329 356.1135 338.1030 176.0707	

Table 3

Chromatographic and ESI-TOF data of hydrastine and proposed metabolites in urine from healthy volunteers following oral administration of 2.7 g of goldenseal supplement (equivalent to 78 mg hydrastine).

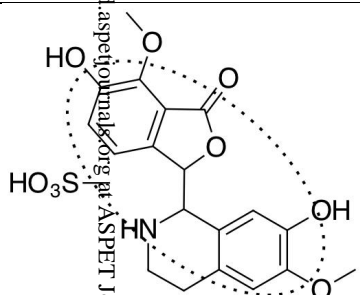

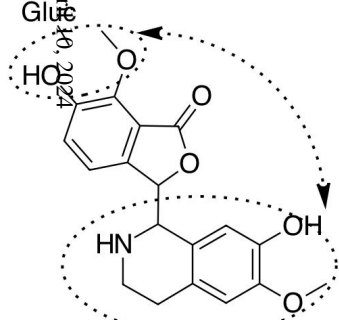
ID	Proposed Reaction	t _R (min)	Expected ion (m/z)	Measured ion (m/z)	Formula	Peak area*	%Hydrastine	MS/MS fragments (m/z)	Proposed Structure
M 27	C-O reduction, N-demethylation, O-demethylation, O-sulfation	16.9	438.0860	438.0851 (-1.8)	C ₁₉ H ₂₀ NO ₉ S	145±88,	19	358.1266 258.0418 297.0751 178.0871	
M 29	C-O reduction, N-demethylation, O-demethylation, O-sulfation	18.6	438.0860	438.0867 (1.8)	C ₁₉ H ₂₀ NO ₉ S	48±26,	6	358.1269 178.0868	
M 30	C-O reduction, N-demethylation, O-demethylation, O-glucuronidation	12.7	534.1612	534.1601 (-2.1)	C ₂₅ H ₂₈ NO ₁₂	74±73,	10	516.1489 358.1084 340.1005 178.0872	

Table 3

Chromatographic and ESI-TOF data of hydrastine and proposed metabolites in urine from healthy volunteers following oral administration of 2.7 g of goldenseal supplement (equivalent to 78 mg hydrastine).

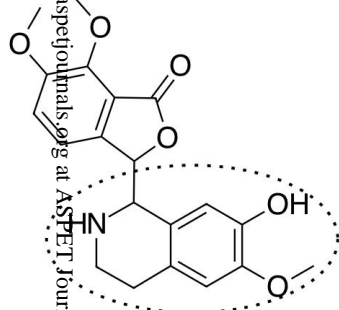
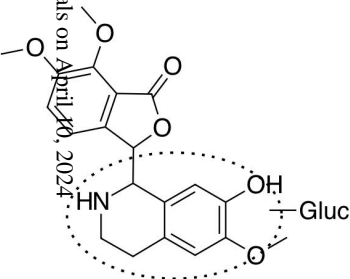
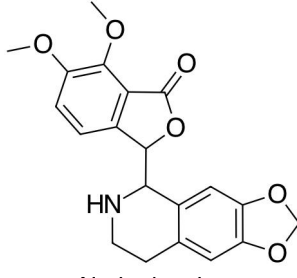
ID	Proposed Reaction	t _R (min)	Expected ion (m/z)	Measured ion (m/z)	Formula	Peak area*	%Hydrastine	MS/MS fragments (m/z)	Proposed Structure
M 31	N-demethylation, C-O reduction	31.2	372.1447	372.1447 (0)	C ₂₀ H ₂₂ NO ₆	280±128,	36	354.1348 178.0875 323.1196	
M 32	N-demethylation, C-O reduction, O-glucuronidation	16.7	548.1768	548.1755 (-2.4)	C ₂₆ H ₃₀ NO ₁₂	579±489,	75	M32: 372.1442 354.1183 178.0866	
M 33		17.3		548.1753 (-2.7)		240±108,	31	M33: 372.1435 354.1173 178.0865	
M34	N-demethylation	34.3	370.1290	370.1300	C ₂₀ H ₂₀ NO ₆			176.0796 321.1010 352.1186	

Table 3

Chromatographic and ESI-TOF data of hydrastine and proposed metabolites in urine from healthy volunteers following oral administration of 2.7 g of goldenseal supplement (equivalent to 78 mg hydrastine).

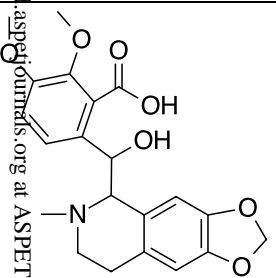
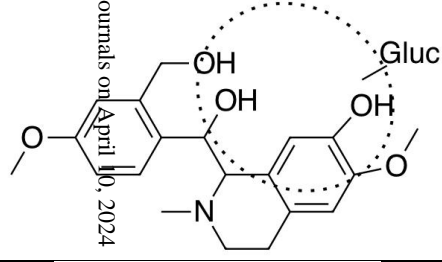
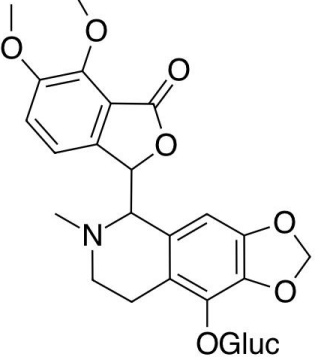
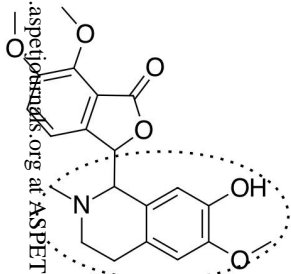
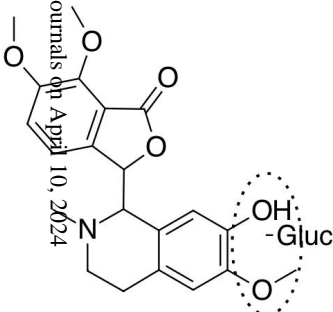
ID	Proposed Reaction	t _R (min)	Expected ion (m/z)	Measured ion (m/z)	Formula	Peak area*	%Hydrastine	MS/MS fragments (m/z)	Proposed Structure
M 36	Lactone hydrolysis	34.0	402.1553	402.1543 (-2.5)	C ₂₁ H ₂₄ NO ₇	329±209,	28	384.1447 366.1384 353.1024 335.0919 323.0924	
M 37	Lactone hydrolysis, C-O reduction, O-glucuronidation	15.9	580.2030	580.2019 (-1.9)	C ₂₇ H ₃₄ NO ₁₃	768±504,	100	562.1642 404.1642 386.1659 368.1326 192.1000	
M 39	Hydroxylation, O-glucuronidation	27.7	576.1717	576.1705 (-2.1)	C ₂₇ H ₃₀ NO ₁₃	235±125	38	400.1353 206.0389 451.2171 467.1917	

Table 3

Chromatographic and ESI-TOF data of hydrastine and proposed metabolites in urine from healthy volunteers following oral administration of 2.7 g of goldenseal supplement (equivalent to 78 mg hydrastine).

ID	Proposed Reaction	t _R (min)	Expected ion (m/z)	Measured ion (m/z)	Formula	Peak area*	%Hydrastine	MS/MS fragments (m/z)	Proposed Structure
M 40	C-O reduction	25.8	386.1604	386.1605 (0.3)	C ₂₁ H ₂₄ NO ₆	482±246, 5,	62	368.1318 337.1096 325.1057 192.1013	
M 41	C-O reduction, O-glucuronidation	18.4	562.1925	562.1921 (-0.4)	C ₂₇ H ₃₂ NO ₁₂	2389±114 5,	309	386.1584 368.1327 325.1041 192.1028	

*; Peak area was the chromatographic peak area from the extracted ion chromatogram. The extracted ion chromatogram was obtained from the (M+H)⁺ trace ± 0.2 amu.

Table 4

Predicted metabolites of canadine detected in urine following consumption of goldenseal supplement

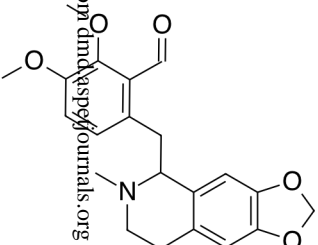
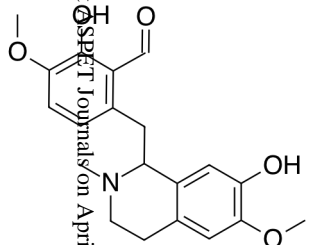
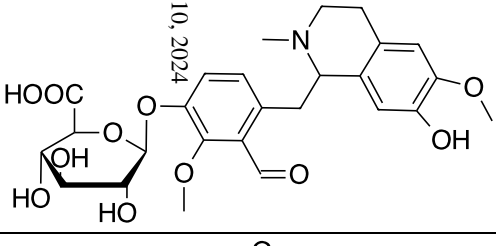
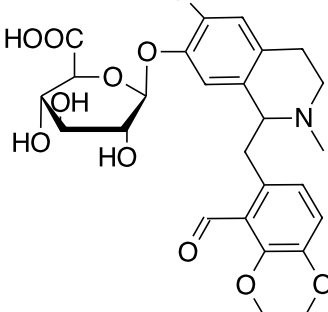
ID	Reaction	t _R (min)	Expected ion (m/z)	Measured ion (m/z)	Formula	Peak area	MS/MS fragments (m/z)	Proposed structure
Canadine		41.6	370.1654	370.1656 (0.5)	C ₂₁ H ₂₃ NO ₅	470,	190.0868	
M43	C-O reduction, O- demethylation	35.1	358.1654	358.1651 (-0.8)	C ₂₀ H ₂₄ NO ₅	177±79, 311	340.1559 192.1015	
M44	C-O reduction, O- demethylation, O- glucuronidation	18.9	534.1975	534.1969 (-1.1)	C ₂₆ H ₃₂ NO ₁₁	29±24, 50	358.1 192.1	
M45	C-O reduction, O- demethylation, O- glucuronidation	24.8	534.1975	534.1959 (-3.0)	C ₂₆ H ₃₂ NO ₁₁	18±11, 31	358.1 354.1 178.1	

Table 4

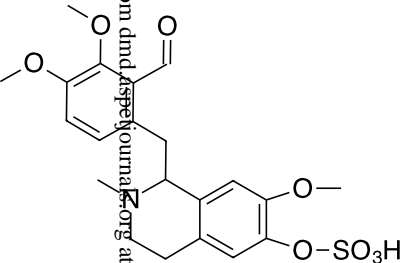
Predicted metabolites of canadine detected in urine following consumption of goldenseal supplement

ID	Reaction	t _R (min)	Expected ion (m/z)	Measured ion (m/z)	Formula	Peak area	MS/MS fragments (m/z)	Proposed structure
M46, M47	C-O reduction,	33.3 33.7	372.1811	372.1809 (-0.5)	C ₂₁ H ₂₆ NO ₅	106±39, 186; 136±68, 225	192.1 272.1 354.1	
M48 M49	C-O reduction, O- glucuronidation	24.5, 27.0	548.2132	548.2111 (-3.8) 548.2117 (-2.7)	C ₂₇ H ₃₄ NO ₁₁	128±68, 225; 549±285, 964	372.1809 368.1339 192.1034	

Downloaded from https://pubs.rsc.org at University of California on April 10, 2024

Table 4

Predicted metabolites of canadine detected in urine following consumption of goldenseal supplement

ID	Reaction	t_R (min)	Expected ion (m/z)	Measured ion (m/z)	Formula	Peak area	MS/MS fragments (m/z)	Proposed structure
M50	C-O reduction, O-sulfation	33.3	452.1379	452.1360 (-4.5)	$C_{21}H_{26}NO_8S$	500±268, 877	372.1799 354.1687 272.0598 192.1031	

Downloaded from dmd.aspetjournals.org at ASPET Journals on April 10, 2024

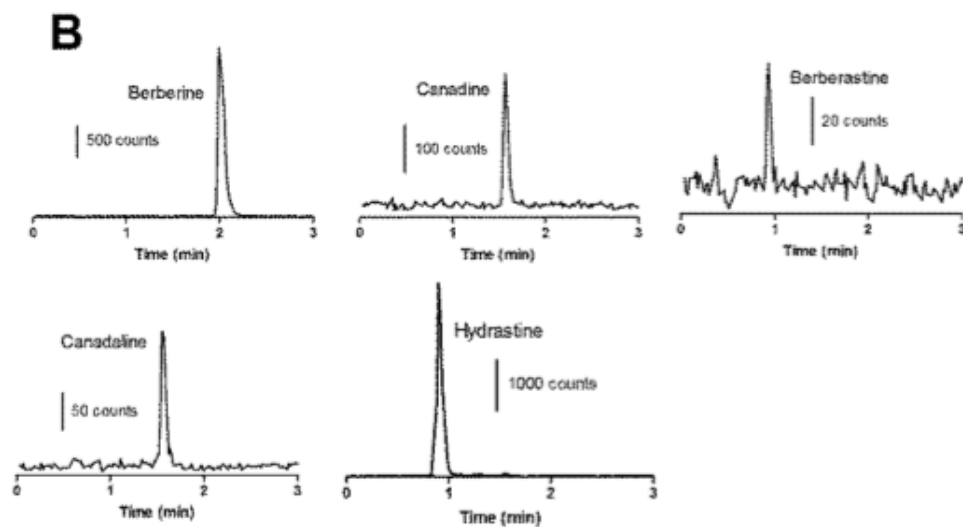
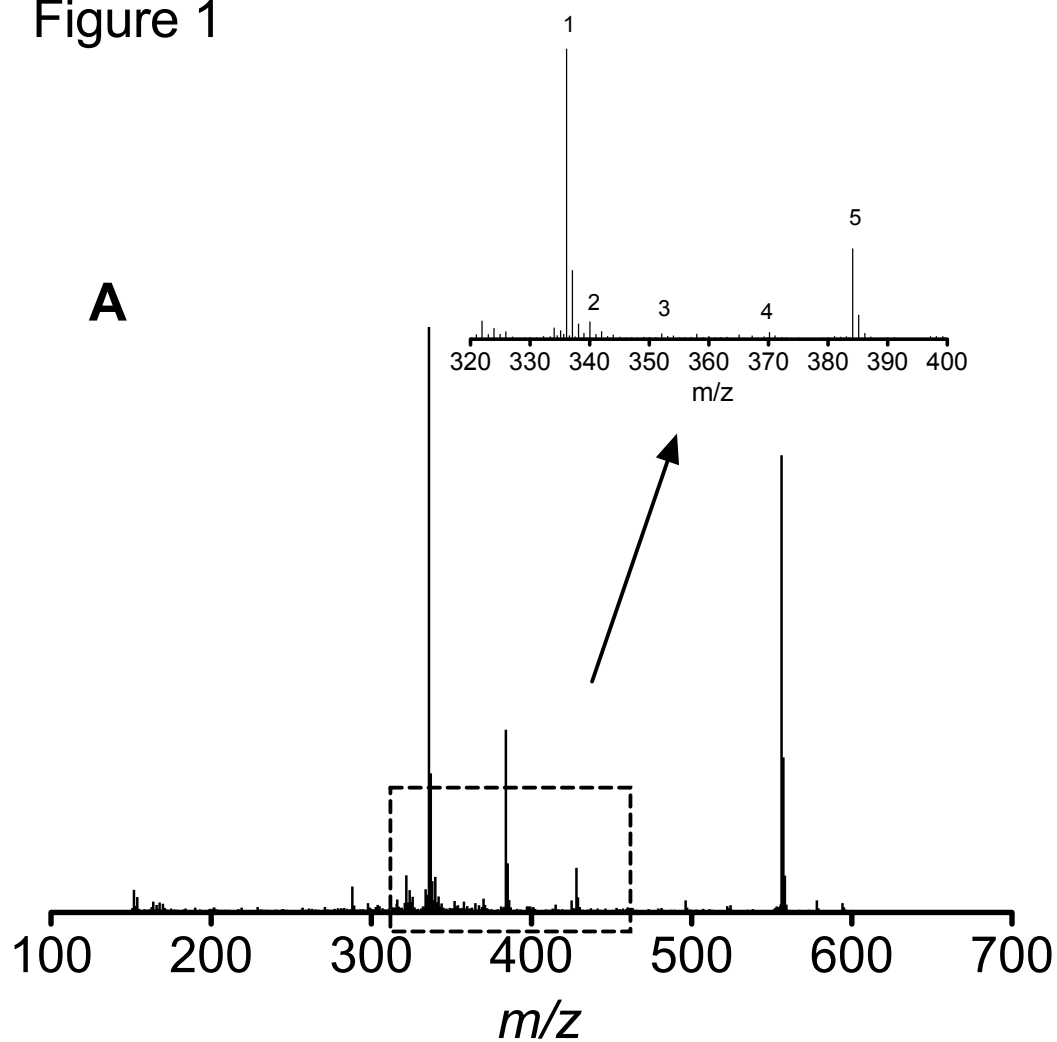
Table 5

Area under the chromatographic peak area versus time and elimination half-life curve for each serum metabolite.

ID	<i>m/z</i>	AUC (Peak Area × h)*	T _{max} (h)	t _{1/2} (h)	Proposed Structure
Hydrastine	386	6435 ± 3027	1.2±0.3	4.8±1.4	
M1 (Hydrohydrastinin)	192	6966 ± 4381	1.4 ± 0.3	22 ± 18	
M36	402	2745 ± 1759	1.2 ± 0.4	5 ± 2	
M41	562	7797 ± 7924	3.0 ± 1	11 ± 15	

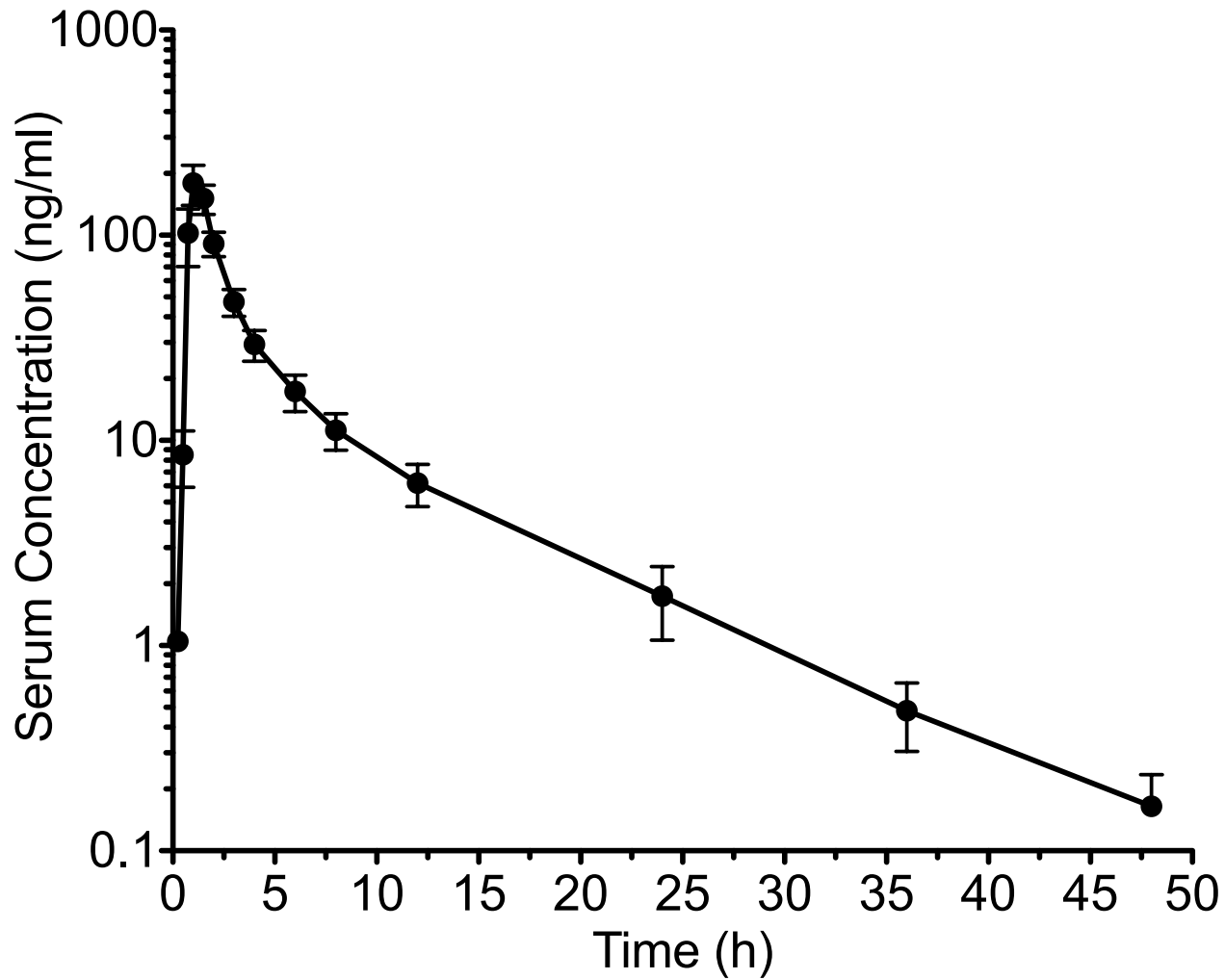
DMD #59410

Figure 1



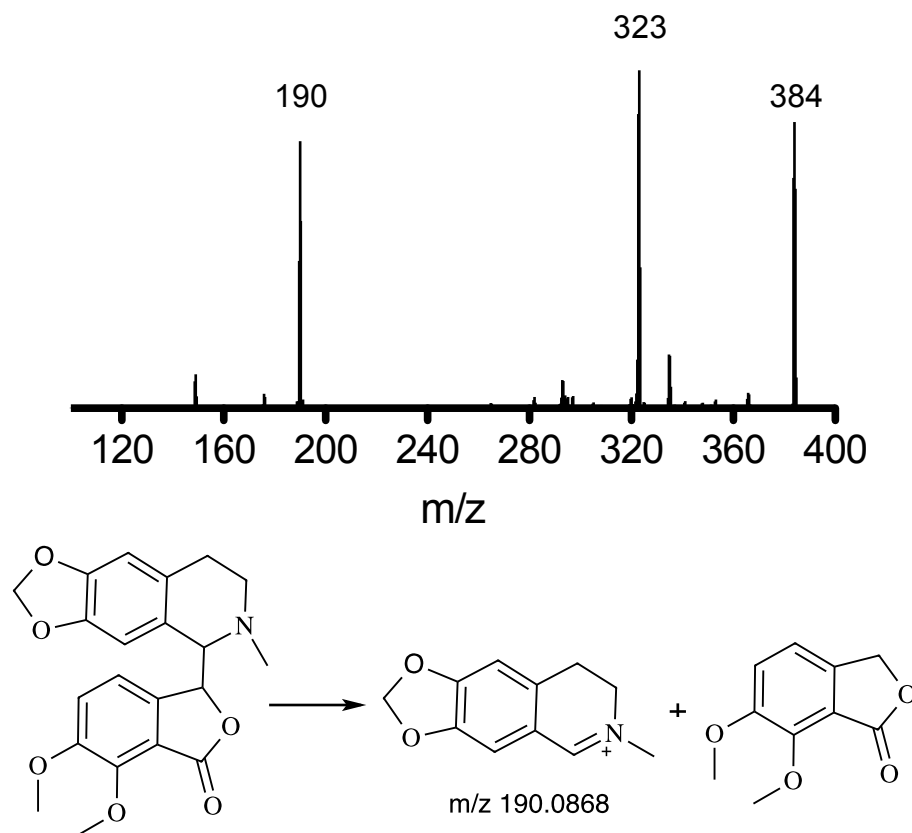
DMD #59410

Figure 2



DMD #59410

Figure 3



DMD #59410

Figure 4

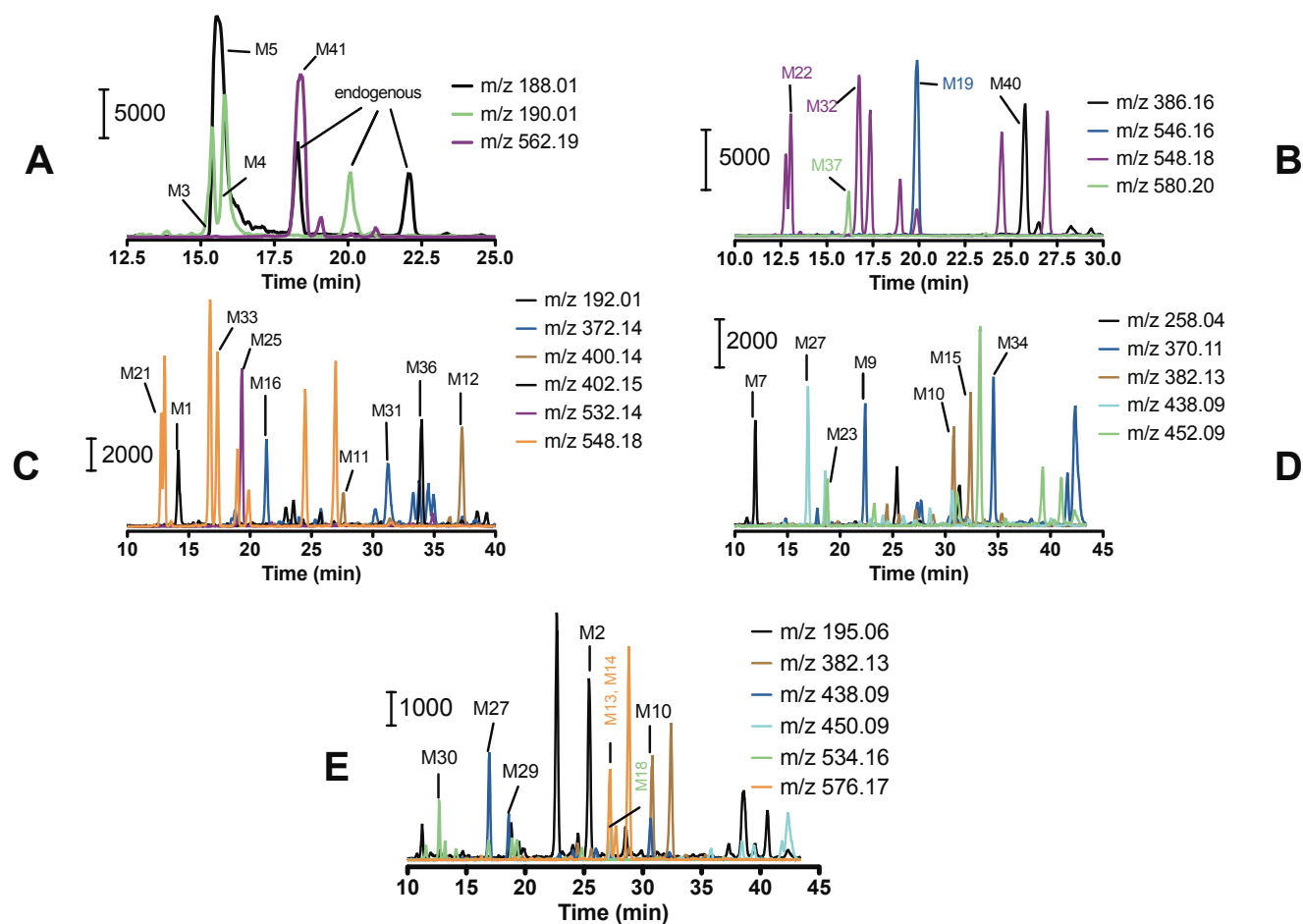


Figure 5

